Research on Engineering Structures & Materials
www.jresm.org
Research Group

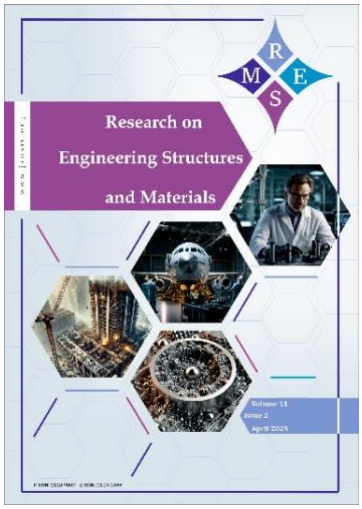

Predicting load-deflection behavior in reinforced concrete beams via the Schnobrich analytical framework

Kamal Alogla

Online Publication Date: 10 June 2026

URL: http://www.jresm.org/archive/resm2026-1663me0510rs.html
DOI: http://dx.doi.org/10.17515/resm2026-1663me0510rs

Journal Abbreviation: *Res. Eng. Struct. Mater.*

To cite this article
Alogla K. Predicting load-deflection behavior in reinforced concrete beams via the Schnobrich analytical framework. *Res. Eng. Struct. Mater.*, 2026; 12(3): 2045-2058

Research on Engineering Structures & Materials
www.jresm.org

Research Article

Predicting load-deflection behavior in reinforced concrete beams via the Schnobrich analytical framework

Kamal Alogla [*,a]

Department of Civil Engineering –College of engineering- Kerbala University, Karbala 56001, Iraq

Article Info

Article History:

Received 10 May 2026

Accepted 09 Jun 2026

Keywords:

Reinforced concrete beams;
Load-deflection prediction;
Schnobrich analytical framework;
Non-associated plasticity;
Smeared crack modeling

Abstract

The Schnobrich model used to predict the load-deflection behavior of reinforced concrete (RC) beams under monotonic loads is improved in this study. The accuracy of these improvements is validated by applying the model to two composite beams that had previously been tested and the results compared to theory. Comparisons are made with code limit state design approaches (ACI 318-19; AISC, 2017). The Schnobrich model utilizes a combination of non-associated plasticity, smeared cracking, and other incremental constitutive laws, and in each case exceeds the predictability of both codes, with AA% of 97.62% and 93.03%, as compared to 95.36% and 92.87% respectively. Key statistical results (e.g., RMSE: 2.43 kN Vs 4.46 kN; R^2: 0.9977 Vs 0.9922) indicate the model's ability to capture highly nonlinear phenomena such as stiffness degradation, and behavior after yielding. The modified model thus is considered highly effective in achieving feasible, reliable, and accurate predictions, thereby validating its adoption and enhancing its potential applicability to real-life RC beam design problems, thus providing a better link between code-based approaches and more complicated numerical approaches.

1. Introduction

Reinforced concrete (RC) beam characteristics related to loading behavior (and hence deflection) are essential for safe and effective long-term performance in the field of structural engineering. It is crucial to anticipate how a reinforced concrete beam will perform when subjected to changing loading configurations over time and will also perform when subjected to other types of loads in different locations on the same beam [1,2]. Material models for analysis of these beams traditionally rely on linear-elastic stress-strain constitutive relationships for steel and concrete with elastic-perfectly plastic behavior for both materials [3]. Traditional analysis is still very much in use for quick designs or code checks while Finite Element Analysis (FEA) is more suited to detailed numerical solutions [3-5].

Composite beam configurations demonstrate complex load-deflection behaviors when compared with conventional RC beam configurations. The load-deflection characteristics of composite beam configurations depend on the interaction that occurs between the concrete in the composite configuration and the structural component embedded or attached to it (e.g., a steel profile or a GFRP element). The load transfer mechanism for steel-concrete composite beams relies heavily upon the interaction that occurs between the two materials and affects the overall stiffness, the rate at which cracking progresses, the yield behavior, and the ultimate load capacity of the composite beams. Similarly, for GFRP-concrete composite beams, the stiffness will deteriorate at a different rate, the bond behavior will be different, and the behavior after cracking will also be different when compared with conventional RC beam designs due to the differences in mechanical properties of GFRP as compared with traditional composite materials. The analysis presented in

*Corresponding author: kamal.d@uokerbala.edu.iq
[a]orcid.org/0000-0002-0853-5152
DOI: http://dx.doi.org/10.17515/resm2026-1663me0510rs

this paper will validate the enhanced Schnobrich analytical framework for two different composite beam configurations (B1 being the steel-concrete composite beam and B2 being the GFRP-concrete composite beam) thereby establishing the boundaries of the current research and differentiating the behavior of the composite beam configurations being researched from the behavior of traditional RC beam configurations.

Code-based standard procedures for the design of concrete and composite steel structural members (e.g., the ACI 318-19 and AISC 2017 codes, respectively) are predominantly used to determine the flexural response, serviceability deflection, and ultimate strength of the structural member being designed. These codes are focused primarily on providing a safe and simplified method of checking the design of the structural member, as opposed to providing a detailed analytical method for simulating the complete nonlinear load-deflection response of the member. Therefore, the code-based calculations will not include adequate representation of factors such as stiffness degradation, crack growth, yielding, bond behavior, and post-cracking behavior for composite beam systems; thus, the need for a more detailed analytical method, such as the Schnobrich model, exists in order to provide a more accurate representation of the load-deflection behavior that has been observed experimentally.

There have been many mechanisms to predict the nonlinear response of RC and composite beam structures such as the Schnobrich model. The Schnobrich model was mainly used for predicting the response of prestressed concrete structures where the method essentially accounts the material nonlinearity, cracking behavior, and bond-slip effect in the model, which makes it balanced in terms of accuracy and computational complexity among other methods [6]. With respect to serviceability limit state (SLS) check, the model is advantageous over non-linear models, since it considers the degradation in stiffness due to crack opening and yielding of reinforcements to a limited extent as opposed to the modelling as perfectly elastic and perfectly plastic representation and also due to the low stiffness to strength ratio of the concrete material [7-9].

The Schnobrich model's applicability has been studied quite a bit. Ali and Forth study showed that the model can properly predict the time dependent deflection behavior of reinforced concrete beams under sustained eccentric loading i.e., bend and torsion [10]. Their study showed the use of the method to account for the stiffness reduction due to creep effect and crack growth which the code is known to underestimate quite a bit (i.e., Eurocode 2). Vecchio and Collins in 1986 combine the Schnobrich model with the Modified Compression Field Theory (MCFT) for modeling of shear and torsion behavior in cracked concrete members [11]. And while there have been many more studies since then, the Schnobrich model is still not calibrated for high strength concrete and fiber reinforced polymer (FRP) strengthened beams where the bond performance and modes of failure are significantly different from conventional RC [12,13].

Further validation for the Schnobrich model has recently been performed using experimental and numerical modeling techniques. Higgins study in 2013 have used large-scale beam tests to verify the Schnobrich model which reasonably predicted post-cracking stiffness and deflection progression [14]. Also, the model has been expanded by Nie and Cai to consider shrinkage-induced curvature which is an important parameter to assess long-term serviceability [15]. Nevertheless, deflection predictions by the Schnobrich model [16] are found to be not enough accurate for high shear-torsion interaction cases where the redistribution of stresses due to incipient-diagonal cracking would exacerbate the deflections [17] which really necessitate a further development of the model ulteriorly in combined loading conditions and non-uniform reinforcement layouts.

The primary purpose of this investigation is to enhance the Schnobrich analytical model to predict the load-deflection response of steel–concrete and GFRP–concrete composite beams under short-term monotonic three-point bending loads. The predicted values from the analytical method are validated against experimental data and against the theoretical predicted values from ACI 318 and the 2017 AISC code for the design of structural steel. The objectives of this research are to (1) evaluate the predictive accuracy of the Schnobrich model for load-deflection predictions of composite beams; (2) compare the results from the Schnobrich model with both actual and code-based prediction values; (3) demonstrate the benefits to engineering of using a nonlinear analytical technique to model cracking, stiffness degradation, and post-cracking behavior. All time-dependent

behavior, such as creep and shrinkage, cyclic behavior, sustained load behavior, shear-torsion interaction, and combined load cases, are excluded from this study.

2. Schnobrich Model

The Schnobrich analytical framework is an indirect (nonlinear) simulation of load-deflection behavior of concrete and composite structural members, taking into account the effects of material nonlinearities, cracking, stiffness degradation, and inelastic deformation. The framework was originally developed at the University of Illinois by Professor William C. Schnobrich as a means to provide a more realistic analytical tool than conventional linear-elastic methods, especially for reinforced concrete structures [16]. The Schnobrich Analytical Framework utilized in this study, allows for an appropriate nonlinear characterization of the monotonic flexural loading behavior of concrete and composite beams. This analytical representation is especially relevant given that the adoption of a non-associated plasticity framework separates the yield function from the plastic potential function, providing a much more representative model of the actual dilatant volumetric expansion of concrete under compression. In addition, the use of smeared cracking permits the distributed effects of cracking to be included in the stiffness formulation rather than treating the cracks as isolated discrete discontinuities. Therefore, the proposed analytical model is capable of predicting the load-deflection response of composite beams in their uncracked, cracked-elastic, yielding and post-cracked stages as defined within this study. No consideration has been given to the cyclic, seismic, creep or shrinkage effects as they are considered to be outside the defined scope of the present study [18].

Moreover, smeared cracking is used to model the distributed characteristics of cracking in concrete as a result of applying smeared cracking to the finite element geometry; cracks are considered to be continuous and part of the matrix, rather than discrete points of failure. In this way, smeared cracking provides the basis for simulating gradually decreasing stiffness and applying tension stiffening effects to post-cracking load redistribution within the model. Therefore, the combination of using smeared cracking and non-associative plasticity provides the theoretical foundation to implement the Schnobrich analytical framework to predict load vs deflection behavior of composite beams in the current study.

Consequentially, a range of mathematical formulations have been heavily substantiated against experimental data, particularly biaxial concrete tests conducted by Kupfer in1969 [19], the results of which are promising in that the model exhibits substantially superior predictive accuracy with respect to associated plasticity models; excellent agreement is demonstrated between theoretical predictions and experimental data illustrating structural response.

3. Hypotheses Based on The Schnobrich Model

The Schnobrich analytical model used in this research relies on a group of consistent model assumptions that establish the boundaries and process of mathematically modeling concrete performance subjected to short-term (monotonic) flexural loads. The model assumptions are grouped in this way [20,21]:

- Non-Associated Plasticity: the non-associated model defines separate yielding and plastic flow mechanisms for concrete, which allows for a more accurate representation of the dilatant (volume-expanding) nature of concrete's behavior under compressive loading. Validation of this model has been found through experimental results from study of Kupfer providing better prediction of the stress-strain and volumetric responses of concrete compared to the other models discussed above [19].
- Plane Stress Assumption: in the modelling of structural members subjected to two-dimensional (2D) plane stress loading, we make use of simplified 2D stress state assumptions and therefore, we have applied these assumptions to several different structural members, such as slabs, beams and walls, without significant reduction in the accuracy of our predictions [21].

- Strain-Hardening Behavior: due to the fact that concrete will initially harden elastically and subsequently soften, we can develop realistic post-yield response behavior based on the plastic work that a member has experienced [20].
- Monotonic Loading: do not model the effects of creep or cyclic behavior on short term monotonic loads.
- short-term loads represent static or quasi-static loading, thus allowing for increased computational efficiency [21].
- Incremental Constitutive Relations: stress-strain relationships are developed on an incremental basis, allowing these stress-strain relationships to be incorporated into finite element analysis while ensuring consistency with the results obtained from the experimental testing of concrete [20].
- Distribution of Damage and Cracks: Cracks are shown to be a form of distributed damage in the concrete continuum. The after-cracking behavior is determined by the assumptions for tension-stiffening and shear-retention, which correspond to the gradual reduction in stiffness that occurs after cracking has occurred [21].
- The Yield Function for Concrete Developed by Hu and Schnobrich [20] :defines the multiaxial plastic yield threshold of concrete as a function of its first stress invariant (I1) and second deviatoric stress invariant (J2). In effect, this formulation describes the pressure dependency of yielding for Concrete in an appropriate multiaxial stress environment.
- Plastic Potential: A Drucker–Prager-type potential governs flow direction, incorporating a dilatancy parameter to model volumetric expansion in plasticity [20].

The success of these hypotheses to predict load–deflection response of reinforced concrete beams during complicated loading is one of the factors that collectively underwrite the predicted performance of the Schnobrich Framework.

4. Methodology and Mathematical Formulation of Design Codes for Composite Sections

For a rigorous estimation of deflection in composite beam systems, this research incorporates the design provisions in both concrete and steel design codes. The analysis methodology includes the necessary transformational stress checks (elastic) of the primary concrete and steel components using the procedures based on ACI 318-19 (American Concrete Institute, 2019) [22] using un-cracked transformed sections and cracked transformed sections which were given in the ACI 318-19 (ACI 2019) provisions code for reinforced concrete member. The transformed-section technique (modular ratio) refers to a method where the steel part of a composite (steel-concrete composite section) is transformed into an equivalent concrete cross-section based off of the elastic modulus of the two materials. The modular ratio is defined as n = E s/E c, where E s is the elastic modulus of steel and E c is the elastic modulus of concrete. For a composite beam made of GFRP and concrete, the same concept of equivalent areas will be applied through a modulus ratio between the GFRP element and the concrete element. The result of the transformation is that during the elastic and cracked-elastic stages of the beam, the composite section may be analyzed the same way as if it were a homogeneous section. The same plastic stress distribution methodology of AISC 2017 (American Institute of Steel Construction, 2017) [23] for composite section was used for the ultimate strength behavior of the steel-concrete composite members and the internal moment capacity.

The proposed code-based analytical procedure uses material properties along with information about the elastic and plastic limits to develop an accurate estimate of deflection for a composite section of steel and concrete at various loads. The responses of these beams will depend on three different behavioral phases: uncracked elastic behavior, cracked-elastic behavior and ultimate capacity.

Stage limits have defined the transition from elastic analysis (using ACI) to a plastic stress distribution (using AISC). In the first stage of the analysis, the member was considered an uncracked transformed section until the applied moment level reached the cracking level M cr (i.e., the cracking moment). Once the member was considered cracked, the analysis was performed

again with the cracked transformed section properties, demonstrating the cracked elastic phase of the member, and reduced stiffness. The transition to the ultimate capacity stage occurred either when the yield strain of the tensile steel was reached (εy=fy/Es) or when the extreme concrete compression strain approached the selected ultimate strain (εcu). At this point, the ultimate moment capacity of the composite section was determined through the AISC plastic stress distribution method. Therefore, the combined ACI/AISC approach was used as a staged process instead of substitutive simultaneous using the formulations from one code into another.

To estimate mean deflection at any load, a combined approach uses ACI 318-19 for elastic analysis of uncracked and cracked sections, and AISC 2017 for the plastic moment capacity of composite beams [22,23]. Deflection for the uncracked section relies on gross section properties, while for cracked sections, a weighted average of gross and cracked moments of inertia is used, reflecting stiffness reduction as cracking progresses. At each load step, moments and deflections are updated and compared to experimental data for model validation.

$$y_{max} = \frac{P.L^3}{48.E_c.I_g} \quad for\ uncracked\ section \tag{1}$$

$$y_{max} = \frac{P.L^3}{48.E_c.\left\{\left[\left(\frac{M_{cr}}{M_a}\right)^3.I_g\right] + \left[1-\left(\frac{M_{cr}}{M_a}\right)^3\right].I_{cr}\right\}} \quad for\ cracked\ section \tag{2}$$

In this context, P is the applied load, L is the span length of the beam, Ec is elastic modulus of concrete, Ig is gross moment of inertia, and Ie is the effective moment of inertia for the cracked section. Ma denotes the bending moment for any applied load La, while Mcr represents the moment when cracking begins. Ig is the moment of inertia of the gross (i.e., uncracked) section. I_cr is the moment of inertia of the cracked section. The major variable in calculating the moment at a specific load increment. However, the moment will be evaluated at successive intervals for each load increment in order to calculate an average value.

5. Materials and Sample Preparation

The evaluation of reliability and predictive accuracy of the proposed analytical framework is an important aspect of this study. Therefore, closed-cell beam specimens with available experimental test data have been reanalyzed and used to verify the accuracy of the analytical framework. The test specimens were previously tested under three-point bending conditions with simply supported beams; these specimens were drawn from previous experimental studies conducted by Li in 2012 and Ibrahim in 2023 [24,25].

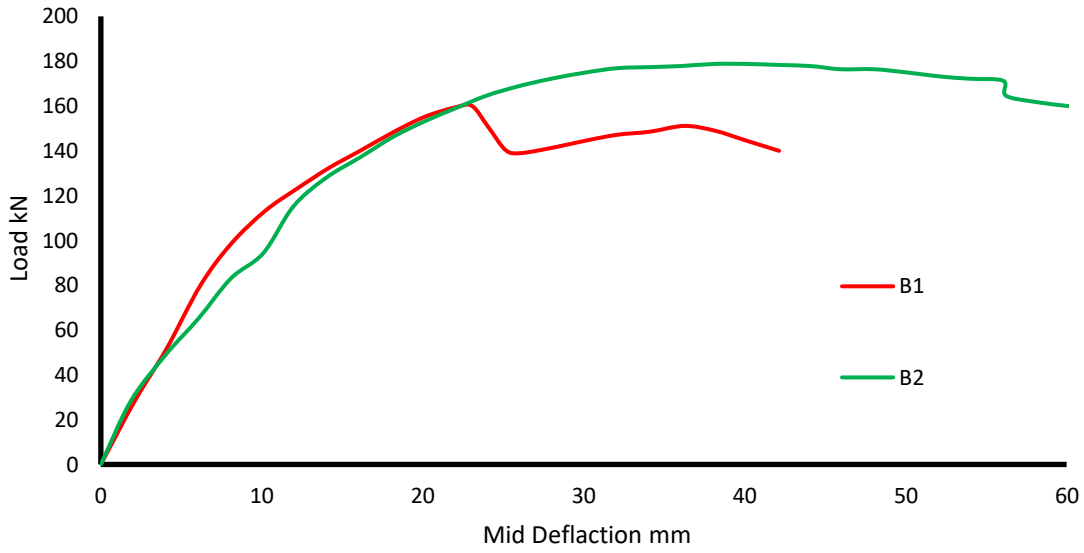

Fig. 1. Load–mid-deflection response of the tested composite beam specimens

Table 1 provides an overview of the basic material properties of the beams, as well as other significant aspects that characterize them. The italicized values in Table 1 are approximations based on the lack of experimental test data. They are based on comparable structural configuration benchmarks found within literature and general practices throughout structural engineering.

The two case studies on beams have been divided into 2 categories; Beam B1 is part of an experimental program published by Li [24] and Beam B2 is part of a research project by Ibrahim [25]. Both specimens were tested under a simply supported three-point bending configuration, and the corresponding load–mid-deflection response was used for model validation.

Table 1. Material properties and Geometrical of steel–concrete beam analyzed

No.	Property	Unit	Beam	
			B1 Li et al. [24]	B2 Ibrahim et al. [25]
1	Concrete beam width, bc	mm	160	200
2	Concrete beam thickness, hc	mm	250	300
3	Steel section height, h_s	mm	140	150
4	Steel section web thickness, tw	mm	5.5	10
5	Steel flange width, bs	mm	80	100
6	Steel flange thickness, tf	mm	9.1	10
7	Reinforcement cover	mm	40	40
8	Tension steel area, As	mm^2	85	157
9	Compression steel area,A′s	mm^2	57	402
10	Beam span length, L	mm	2000	2750
11	Shear span under central point load, a=L/2	mm	**1000**	**1375**
12	Concrete strength, f′c	MPa	48.4	25.75
13	Concrete ultimate strain, εcu	-	0.002	0.002
14	Concrete elastic modulus, Ec	GPa	33.23	23.98
15	Concrete cracking strain, εt=ft/Ec	-	0.000144	0.000116
16	Concrete tensile strength, ft	MPa	4.8	2.78
17	Steel elastic modulus, Es	GPa	200	200
18	Steel yield stress, fy	MPa	276	315
19	Steel yield strain, ε_y	-	0.02	0.02
20	Steel strain corresponding to its ultimate strength, ε_{su}	-	0.03	0.03
21	Steel profile yield strength, fsy	MPa	315	520.7
22	Steel profile ultimate strength, fsu	MPa	410	600

6. Mathematical Models of The Schnobrich Analytical Framework

The Schnobrich Analytical Framework is an important milestone in the use of mathematical modelling to assess the performance of reinforced concrete structures, especially their capacity to resist complex loads and the resulting deflection behavior. The structure of this system includes an innovative mathematical model to clarify the distinction between classical forms of plasticity theory and their applications to reinforced concrete. This was accomplished by adding some of the distinct characteristics of non-associative plasticity principles, which were created specifically for concrete materials.

Schnobrich model uses mathematics to indicate that concrete behaves differently than metal. Therefore, the analysis of plastic behavior in concrete or other materials requires the development of new models (e.g., Schnobrich) that do not relate directly to pure metal plasticity models. The Non-Associated Plasticity Theory provides an opportunity for more accurately modeling the volume change(dilatant) behavior of concrete and is based on the decoupled yield function and plastic potential function for concrete [16,20,21]. The additive decomposition of rates of deformation (strain) makes up the majority of these mathematical models:

$$\dot{\varepsilon}=\dot{\varepsilon}e+\dot{\varepsilon}p \quad (3)$$

In addition to providing the means for distinguishing between the elastic strain ε̇e and plastic strain ε̇p rates, it characterizes both elastic and plastic performance of concrete.

6.1 The Hu-Schnobrich Yield Function

The mathematical foundation of the framework is the Hu-Schnobrich yield function. This yield function uses extensive experimental validation through biaxial concrete test data to develop it as an analytical function [20]:

$$f(\sigma,\kappa)=\alpha I1+\sqrt{J_2}-k(\kappa)=0 \quad (4)$$

Where;

- f(σ,κ) is the yield function that defines the plastic yielding condition of concrete under multiaxial stress states.
- α *is a material parameter that controls the pressure sensitivity of the yield function.*
- I_1 is the first stress invariant, representing the hydrostatic stress component.
- J_2 is the second invariant of the deviatoric stress tensor, not a material parameter.
- $k(\kappa)$ is the hardening/softening function, which depends on the internal variable k.

This formulation effectively captures concrete's pressure-dependent behavior, providing superior accuracy compared to traditional von Mises criteria developed for metallic materials.

6.2 Non-Associated Flow Rule

The framework employs a non-associated flow rule that mathematically separates the direction of plastic flow from the yield surface orientation [20,21]:

$$\dot{\varepsilon}^{p} = \dot{\lambda}.\frac{\partial g}{\partial \sigma} \quad (5)$$

The plastic strain-rate tensor, ε̇p, is defined mathematically by using the following equation: ε̇p = λ̇ ∂g/∂σ in which ε̇p is the plastic strain-rate tensor, λ̇ is the plastic multiplier, g is the plastic potential function, and ∂g/∂σ is the gradient of the plastic potential function with respect to the stress tensor σ. In this case, the use of a flow rule that is non-associated means that the plastic potential function g and the yield function f are different. Therefore, the direction of plastic flow can be defined independently from the yield surface (i.e., the yield surface is independent of plastic flow). Plastic potential functions are generally defined using the Drucker-Prager [20,21] formulation:

$$g=\beta I_1+\sqrt{J_2}-c=0 \quad (6)$$

Where β is the dilatancy parameter controlling volumetric plastic strain development, and c is a material constant.

6.3 Constitutive Relations and Incremental Formulation

The mathematical framework employs incremental constitutive relationships to handle nonlinear behavior:

$$d\sigma=Dep:d\varepsilon \quad (7)$$

The elasto-plastic stiffness matrix is mathematically expressed as [20,21]:

$$D^{ep} = D^{e} - \frac{\left(D^{e}:\frac{\partial f}{\partial \sigma}\right)*\left(\frac{\partial g}{\partial \sigma}:D^{e}\right)}{H+\frac{\partial f}{\partial \sigma}:D^{e}:\frac{\partial g}{\partial \sigma}} \quad (8)$$

De is the Elastic stiffness package, H is your hardening modulus, ∂f/∂σ is the yield function gradient with regard to your stress tensor, and ∂g/∂σ is the plastic potential function's derivative with regard to the stress tensor. When employing the Dyadic Product Operator within both the Elasto-Plastic Kinematic Stiffness and Elasto-Plastic Flow Stress will result in a product of those two

respective elastic tensor terms as well as any other state variables relevant to each of those particular state representations.

6.4 Hardening and Softening Laws

The mathematical treatment of material hardening incorporates strain-hardening behavior through the evolution equation [16,20,21]:

$$\dot{\kappa}=\dot{\lambda}h(\sigma,\kappa) \tag{9}$$

For concrete applications, the hardening parameter is often related to the accumulated plastic work:

$$\kappa = \int_0^t \sigma : \dot{\varepsilon}^p . dt \tag{10}$$

This formulation enables the model to capture the progressive stiffening of concrete approaching the yield surface, followed by controlled degradation in the post-yield range.

6.5 Consistency Conditions and Numerical Implementation

The mathematical framework includes consistency conditions ensuring stress states remain on the yield surface during plastic loading [20,21]:

$$\dot{f} = \frac{\partial f}{\partial \sigma} : \dot{\sigma} + \frac{\partial f}{\partial \kappa} . \dot{\kappa} = 0 \tag{11}$$

For numerical implementation, the framework employs implicit integration schemes with convergence criteria:

$$|| R_i || \leq \epsilon_{tol} || R_0 || \tag{12}$$

Where R_i represents the residual vector at iteration i, ensuring numerical stability and accuracy.

6.6 Cracking and Post-Cracking Behavior

Concrete cracking can be mathematically modelled using a smeared cracking model. The smeared cracking model treats cracking effects as being distributed throughout a continuum, in this case the finite element mesh, and accounts for tension stiffening properties through the use of modified constitutive equations [16,20,21]:

$$\sigma=Dcr:\varepsilon \tag{13}$$

Where Dcr represents the cracked concrete stiffness matrix, accounting for reduced tensile capacity while maintaining shear retention across crack surfaces.

7. Application To Load-Deflection Analysis (Schnobrich Models and Codes)

Three separate phases exist when developing full load-deflection curves using the Schnobrich Method. The first phase is the uncracked and elastic stage; therefore, an uncracked element's response is affected primarily by the elastic modulus and gross section stiffness. The second phase is the cracked and elastic stage; therefore, an effective moment of inertia can be used to represent the gradual decline in stiffness due to cracking. The third phase is the post-yield, non-linear stage; therefore, hardening, softening, and degradation of stiffness will all have a significant effect the overall behavior of the element [20,21].

Integrating the three phases of the model gives us an accurate prediction of all phases of behavior from initial loading to a complete failure. Thereby, making the framework practical in both research and engineering-design applications. The present study has performed two independent analyses. The first was a nonlinear analysis to establish a load-deflection response that used the Schnobrich analytical framework and the second was a theoretical code-based load-deflection response that was established with ACI 318-19 and AISC 2017 equations. Both methods have created an

independent set of measures that were then individually compared to the experimental load-deflection data for Beams B1 and B2.

The proposed mathematical formulation was designed to be efficient in its computations, while still being physically sound. When using finite element programs to implement this Framework, special care must be taken in handling the non-associated flow rule to ensure stable convergence during the advanced cracking and yielding stages considered in the present monotonic bending analysis.

8. Analysis of the Results Beams B1

For illustrative purposes, the detailed analysis procedure is provided for Beam B1, with Beam B2 assessed analogously and only the final outcomes summarized. The properties of Beam B1 are as previously described, and its load–deflection behavior is depicted in Figure 2 [24], that represents the results of the practical experiment of the model.

Using the model equations, strain values were extracted, and values were applied at each load value in the three phases: elastic, elasto-plastic, and plastic in the equations of the previously mentioned code. The load-deflection curve was obtained by applying equations 12 and 13. In addition, the equations in the ACI 318-19, and AISC 2017 codes were applied to find the load-deflection curve for comparison with the experimental results and the results extracted from the model, as shown in Figure 2, and Table 2 which shows the load-deflection curve for the three cases (experiment, code method, and Schnobrich model) [16,20-23].

Table 2. Values of the Uncracked load, Cracked load, and failure load for beam B1 for different analysis methods

Case	Uncracked load		Cracked load		Failure load	
	Load (kN)	Deflection (mm)	Load (kN)	Deflection (mm)	Load (kN)	Deflection (mm)
Experimental	15.2	0.91	25.7	1.83	160.01	23.81
By ACI 318-19& AISC 2017 Codes	16.6	1.09	30.5	2.12	168.18	24.25
By Schnobrich model	15.7	0.88	25.1	1.78	162.95	24.03

As shown in Figure 2 and Table 2, the predicted loads for beam B1 from the ACI 318-19/AISC 2017 code-based method were larger than those observed experimentally at each phase of deflection, namely uncracked, cracked, and ultimate. Specifically, the predicted loads were 16.6 kN versus 15.2 kN (uncracked), 30.5 kN versus 25.7 kN (cracked), and 168.18 kN versus 160.01 kN (ultimate). Therefore, based on the analysis of the sample, these estimated higher loading capacities should not be considered conservative estimates or safety factors; instead, these capacities are non-conservatively over-estimating what may actually have been the experimental loading capacity. It is also important to note that the comparison here is based upon analytical prediction methods to create a load-deflection curve and does not constitute a full safety assessment as prescribed by the design codes, including load factors, resistance factors, and serviceability requirements specified within the respective codes.

The Schnobrich Model, which is based upon Non-Linear Finite Elements and multiple Spring formulations (for Axial-Flexural Interactions) that account for Hysteretic effects, shows a very close correlation (compartmentalized with the different “Conditions”) between Analytical and Experimental results (Uncracked Load = 15.7kN; Cracked Load = 25.1kN; and Failure Load = 162.95 kN; [21]). The data in terms of the three stages showed that the model was able to accurately replicate the measured deflections in all three stages. This indicates that the model has captured all of the key elements that contribute to the nonlinear performance of the structure (such as bond-slip, stiffness degradation and the spread of plasticity) that cannot be fully captured using traditional code approaches.

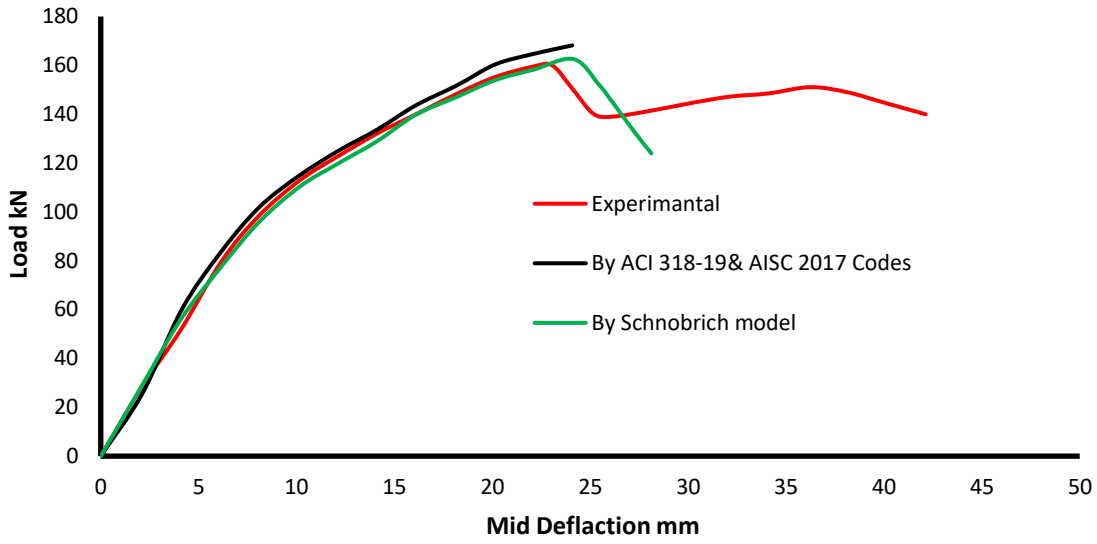

Fig. 2. The response of Beam B1 (Load Deflection) curve

A significant divergence occurs beyond the peak load: The experimental curve exhibits a residual load-carrying capacity and a plateau phase that then gradually declines. This phenomenon indicates that the Schnobrich and code approaches do not completely incorporate all of the effects that could potentially result in strain hardening or the redistribution of pressure on the concrete beam's internal structure following peak loading. The residual behavior may also arise from many different factors, including but not limited to: micro-cracking; the confining pressures to which the concrete is placed; and the post-yield behaviors of the reinforcement; which are often quite difficult to accurately replicate during simulations.

A statistical evaluation of the predictive ability of the ACI318-19 and AISC2017 Code –based model, along with the Schnobrich nonlinear model [20], was made by comparing the model predictions to experimental data as the baseline. In this study, 6 different metrics were used as a basis for comparison. The metrics were used to determine and compare the predictive abilities of the two models (root mean square error (RMSE), normalized root mean square error (NRMSE), mean absolute percentage error (MAPE), coefficient of determination (R^2), and Pearson correlation coefficient (R)).

$$RMSE = \sqrt{\frac{1}{N}\sum_{n=1}^{N}(A_n - P_n)^2} \tag{14}$$

$$NRMSE = \frac{RMSE}{S} \tag{15}$$

$$R^2 = 1 - \frac{\sum(A_n - P_n)^2}{\sum(A_n - S_n)^2} \tag{16}$$

$$MAPE = \frac{\left(\sum\frac{|A-E|}{A}\right) * 100}{N} \tag{17}$$

$$AA\ \% = 100\ \% - MAPE \tag{18}$$

Where (An) actual and predicted (Pn) values and comparing the estimated, (N) number of points within the dataset, (S) normalized against the mean of the actual values.

Table 3 demonstrates that the Schnobrich model outperformed the ACI/AISC code method across all statistical metrics. It recorded a lower RMSE (2.43 kN vs. 4.46 kN) and a smaller MAPE (2.38% vs. 4.64%), leading to a higher AA% of 97.62% compared to 95.36% for the code method. The model also has a better R^2 (0.9977 versus 0.9922), indicating that it explains the variance in the corresponding response variable much more effectively, and a slightly stronger Pearson correlation (R=0.9991 versus 0.9987) that indicates that the model data is an even closer match to the experimental data. Schnobrich and Keshavarzian also indicate that higher accuracy could be

achieved in nonlinear models in capturing the complex behaviours that involve inelasticity and bond-slip, which is not accounted for in the ACI/AISC codes- which are focused on safety and simplicity, rather than simulation or research-level accuracy [20,22].

Table 3. Statistical performance evaluation

Model	RMSE (kN)	NRMSE	MAPE (%)	AA% (%)	R^2	Pearson R
ACI 318-19 & AISC 2017	4.4628	0.0417	4.64	95.36	0.9922	0.9987
Schnobrich Model	2.4252	0.0227	2.38	97.62	0.9977	0.9991

9. Analysis of The Results Beams B2

To help validate the analytical approach to predicting the load-deflection response of composite beams, Beam B2 has been evaluated. An experimental load-deflection curve for Beam B2 was previously reported by Ibrahim et al. [25]. This curve serves as a basis to assess the predicted load-deflection response from both the ACI 318-19/AISC 2017 code procedure and the Schnobrich analytical method. The load-deflection response of Beam B2 (experimental, predicted using code, and predicted using Schnobrich) is illustrated in Figure 3.

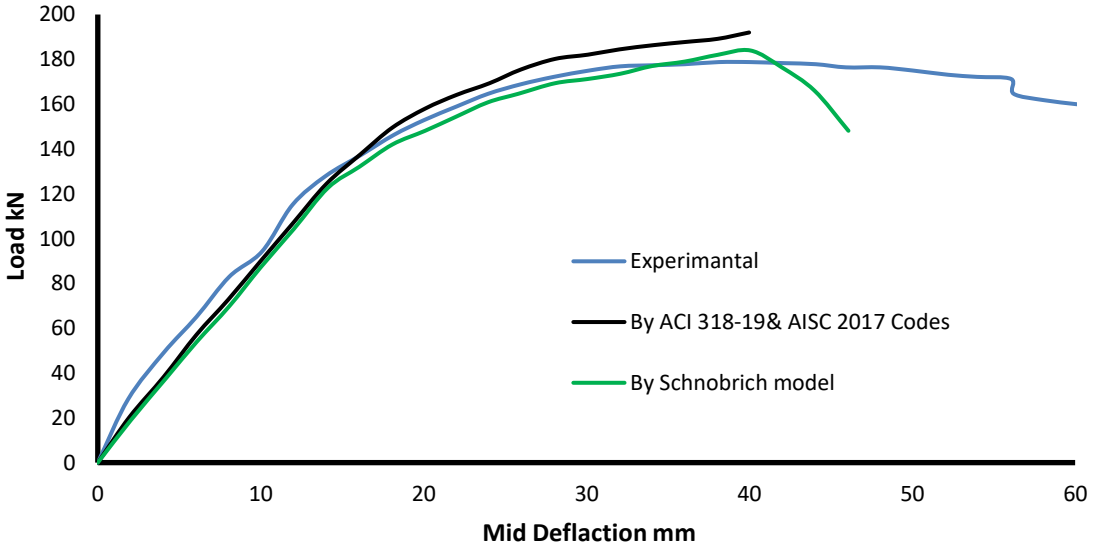

Fig. 3. The response of Beam B2: (Load Deflection) curve

The load–deflection curve for Beam B2 illustrates its flexural behavior under loading, comparing experimental results with predictions from the ACI/AISC codes and the Schnobrich model. In the initial elastic range (up to ~10 mm deflection), all methods exhibit similar trends. However, the Schnobrich model slightly underestimates stiffness, while the ACI/AISC method aligns more closely with the experimental data up to cracking [22,23].

The experimental curves diverged from both models at a deflection of between 10 and 30 millimeters, post cracking to peak load (where the curves peaked). The ACI/AISC methodology clearly overpredicted the load capacity due to code assumptions that were conservative in nature. The Schnobrich model, however, was in better alignment with the experimental curves at peak loads (~175 - 183 kN) and thus better represented non-linear behaviors like redistribution and stiffness degradation (Keshavarzian & Schnobrich, 1985).

After reaching the peak (deflection >35 mm), our experimental results show evidence of softening due to micro-crack formation and the redistribution of strain. The behavior of the models (Schnobrich and ACI/AISC) was not capable of portraying that behavior. The Schnobrich model exhibits a decrease in strength after reaching its peak, while the ACI/AISC model continues to rise sharply after reaching its peak. The response of these models to a post-yielding event indicates that

both models are limited in their ability to model the post-yield behavior of the materials studied [16,20-23]. Ultimately, the Schnobrich model provides the best and most accurate prediction of the failure load behavior of the tested materials, which is consistent with previous studies on advanced nonlinear modelling [21,26].

Table 4. The Uncracked load, Cracked load, and failure load values for beam B2 for three methods

Case	Un-cracked load		Cracked load		Failure load	
	Load (kN)	Deflection (mm)	Load (kN)	Deflection (mm)	Load (kN)	Deflection (mm)
Experimental	20.56	0.96	31.1	2.06	178.77	38.13
By ACI 318-19& AISC 2017 Codes	17.77	1.21	32.7	3.10	191.98	40.20
By Schnobrich model	18.91	1.08	29.8	2.81	183.96	39.88

The experimental, analytical and the Schnobrich Model loads during uncracked, cracked and ultimate failure of the B2 Beam are compared in Table 4 (Comparison of Experimental Data, Code based predictions and Schnobrich Model). This excessive value is regarded as a nonconservative Estimate for the specimen tested, and not a conservative Estimate based on the code. Thus, the code-based curve is specified as an analytical reference only, to reference against, and compare to, the experimental response and Schnobrich model. The Schnobrich model is more accurate than the ACI/AISC method, particularly regarding the prediction for ultimate failure load (183.96 kN). The results indicated that the Schnobrich model is better than the ACI/AISC method in predicting the nonlinear behavior of beams and their flexural response [27].

Table 5. Statistical performance evaluation

Model	RMSE (kN)	NRMSE	MAPE (%)	AA% (%)	R^2	Pearson R
ACI 318-19 & AISC 2017	7.8034	0.0572	7.13	92.87	0.9721	0.9986
Schnobrich Model	6.7378	0.0494	6.97	93.03	0.9792	0.9986

The following Table outlines how well ACI 318-19 and AISC 2017 Methodologies correlate with the Experimental Values in terms of Load/Deflection Response of Beam B2. Both ACI 318-19 and AISC 2017 Methodologies (Pearson R = 0.9986) had a very strong correlation to Experimental Values, yet the Schnobrich Methodology (Predictive Model) was found to provide the Greatest Predictive Accuracy. Although ACI 318-19 and AISC 2017 Methodologies provided Higher RMSE's (7.80 kN) compared to a lower RMSE for the Schnobrich Method (6.74 kN) and a Lower NRMSE for the Schnobrich Method (0.0494), as well as a Small Advantage in MAPE (6.97%), all contributed to a Greater AA% Overall Predictive Accuracy of 93.03%. The Good R^2 Value (0.9792) of the Schnobrich Methodology Further Supports its Greater Predictive Capability.

10. Conclusions

Due to the small number of data points included in the benchmark data set used for comparison purposes, the extent to which we can generalize our results is limited. This study was conducted as an exploratory investigation of the feasibility of using the Schnobrich analysis technique to study specific composite beam subject matter instead of creating a generalizable statistical prediction model. As such, one should be cautious when interpreting the level of correlation between the results from this research and those from the corresponding experimental tests. Future studies should seek to confirm the reliability of the Schnobrich analysis technique through the use of a significantly larger volume of beams, including varying reinforcement ratios; varying shear span to depth ratios; different compressive strength levels of the concrete; different configurations of steel or GFRP reinforcing materials; as well as different combinations of composite material interactions:

- Schnobrich Framework's Predictive Accuracy - The improved Schnobrich framework was able to provide prediction results that are in agreement with experimental outcomes

between 93.03% and 97.62%. The Schnobrich framework also provided an overall higher prediction accuracy than the ACI 318-19/AISC 2017 code-based methods, especially during the nonlinear post-cracking stages, stiffness degradation stages, and at or near ultimate loads.

- The ACI318 - 19/AISC2017 Code Based Predictions overestimated, relative to test specimens, the capacity of the beams for some stages of the study as opposed to an identified safety margin.
- According to a numerical analysis performed with the ACI 318-19/AISC 2017 code-based method, the estimated ultimate load capacities for the subject beams would be overestimated by three to eight percent. Using this information, any difference in actual load–deflection response should be viewed as being non-conservative and not as a safety margin, and therefore, care should be taken in interpreting any code-based analytical prediction compared to actual load–deflection response. Post-Peak Behavior Challenge: Residual load-bearing mechanisms observed experimentally highlight critical gaps in simulating confinement and bond-slip effects for future refinement.

References

[1] Bentz EC, Vecchio FJ, Collins MP. Simplified modified compression field theory for calculating shear strength of reinforced concrete elements. ACI Structural Journal. 2006;103(4):614-624. https://doi.org/10.14359/16438

[2] Hognestad E, Hanson NW, McHenry D. Concrete stress distribution in ultimate strength design. ACI Journal Proceedings. 1955;52(4):455-480. https://doi.org/10.14359/11609

[3] Bazant ZP, Oh BH. Crack band theory for fracture of concrete. Materials and Structures. 1983;16(3):155-177. https://doi.org/10.1007/BF02486267

[4] Abdullatef AD, Ali SI, Aldarraji SYH, Ali MI. Evaluating the Ramberg-Osgood Model for nonlinear moment-curvature analysis of reinforced concrete beams. Research on Engineering Structures and Materials. 2026. https://doi.org/10.17515/resm2026-1518st0217rs

[5] Ali MI, Jamel AAJ, Ali SI. The hardened characteristics of self-compacting mortar including carbon fibers and estimation results by artificial neural networks. In: AIP Conference Proceedings. AIP Publishing LLC; 2020. p. 020159. https://doi.org/10.1063/5.0000177

[6] Al-Rahmani AH, Schnobrich WC. Nonlinear analysis of reinforced concrete shells. Journal of Structural Engineering. 1990;116(3):669-686.

[7] Forth JP, Brooks JJ, Jones AEK. Verification of cracked section shrinkage curvature models. Proceedings of the Institution of Civil Engineers - Structures and Buildings. 2014;167(5):274-284. https://doi.org/10.1680/stbu.12.00046

[8] Jamel AAJ, Ali MI. Stability and seepage of earth dams with toe filter (Calibrated with Artificial Neural Network). Journal of Engineering Science and Technology. 2021;16(5):3712-3725.

[9] Ahmed AM, Ali SI, Ali MI, Jamel AAJ. Analyzing Self-Compacted Mortar Improved by Carbon Fiber Using Artificial Neural Networks. Annales de Chimie - Science des Matériaux. 2023;47(6):347-353. https://doi.org/10.18280/acsm.470602

[10] Ali SA, Forth JP. Time-dependent behaviour of RC beams under eccentric combined loads as a unit of beam-column joint assemblies made from normal strength concrete without/with CFRP wraps. Engineering Structures. 2023;288:116221. https://doi.org/10.1016/j.engstruct.2023.116221

[11] Vecchio FJ, Collins MP. The modified compression-field theory for reinforced concrete elements subjected to shear. ACI Structural Journal. 1986;83(2):219-231. https://doi.org/10.14359/10416

[12] Teng JG, Chen JF, Smith ST, Lam L. FRP-strengthened RC structures. Chichester: Wiley; 2002.

[13] Ali MI, Allawi AA. An Artificial Neural Network Prediction Model of GFRP Residual Tensile Strength. Engineering, Technology & Applied Science Research. 2024;14(6):18277-18282. https://doi.org/10.48084/etasr.9107

[14] Higgins I, Forth JP, Neville A, Jones RC, Hodgson T. Behaviour of cracked reinforced concrete beams under repeated and sustained load types. Engineering Structures. 2013;65:45-56. https://doi.org/10.1016/j.engstruct.2013.05.034

[15] Nie J, Cai CS. Deflection of cracked RC beams under sustained loading. Journal of Structural Engineering. 2000;126(6):708-716. https://doi.org/10.1061/(ASCE)0733-9445(2000)126:6(708)

[16] Schnobrich WC. Design and construction of concrete shells, GS Ramaswamy. International Journal for Numerical Methods in Engineering. 1986;23(4):728-729. https://doi.org/10.1002/nme.1620230415

[17] Peng XN, Wong YL. Experimental study on reinforced concrete walls under combined flexure, shear and torsion. Magazine of Concrete Research. 2011;63(6):459-471. https://doi.org/10.1680/macr.10.00133

[18] Vermeer PA. Non-associated plasticity for soils, concrete and rock. In: Physics of dry granular media. Dordrecht: Springer Netherlands; 1998. p. 163-196. https://doi.org/10.1007/978-94-017-2653-5_10
[19] Kupfer H, Hilsdorf HK, Rusch H. Behavior of concrete under biaxial stresses. ACI Journal. 1969;66(8):656-666. https://doi.org/10.14359/7388
[20] Hu HT, Schnobrich WC. Constitutive modeling of concrete by using nonassociated plasticity. Journal of Materials in Civil Engineering. 1989;1(4):199-216. https://doi.org/10.1061/(ASCE)0899-1561(1989)1:4(199)
[21] Keshavarzian M, Schnobrich WC. Analytical models for the nonlinear seismic analysis of reinforced concrete structures. Engineering Structures. 1985;7(2):131-142. https://doi.org/10.1016/0141-0296(85)90023-9
[22] ACI Committee 318. ACI CODE-318-19: Building code requirements for structural concrete and commentary. Farmington Hills, MI: American Concrete Institute; 2019.
[23] American Institute of Steel Construction. Specification for Structural Steel Buildings (AISC 360-16). Chicago, IL: AISC; 2016.
[24] Li X, Lv H, Zhou S. Flexural behavior of GFRP-reinforced concrete encased steel composite beams. Construction and Building Materials. 2012;28(1):255-262. https://doi.org/10.1016/j.conbuildmat.2011.08.058
[25] Ibrahim TH, Alshaarbaf IA, Allawi AA, Oukaili NK, El-Zohairy A, Said AI. Theoretical analysis of composite RC beams with pultruded GFRP beams subjected to impact loading. Engineering, Technology & Applied Science Research. 2023;13(6):12097-12107. https://doi.org/10.48084/etasr.6424
[26] Golafshani EM, Ashour A. Prediction of self-compacting concrete elastic modulus using two symbolic regression techniques. Automation in Construction. 2016;64:7-19. https://doi.org/10.1016/j.autcon.2015.12.026
[27] Rodríguez L, Linero D. Numerical modeling of plain concrete with finite elements using plasticity theory and the Hu and Schnobrich yield function. Revista Ingeniería de Construcción. 2012;27(3):129-144. https://doi.org/10.4067/S0718-50732012000300002